

Theoretical study of the absorption spectra of the sodium dimer

H.-K. Chung, K. Kirby, and J. F. Babb

Institute for Theoretical Atomic and Molecular Physics,

Harvard-Smithsonian Center for Astrophysics,

60 Garden Street, Cambridge, MA 02138

Abstract

Absorption of radiation from the sodium dimer molecular states correlating to Na(3s)-Na(3s) is investigated theoretically. Vibrational bound and continuum transitions from the singlet $X^1\Sigma_g^+$ state to the first excited $A^1\Sigma_u^+$ and $B^1\Pi_u$ states and from the triplet $a^3\Sigma_u^+$ state to the first excited $b^3\Sigma_g^+$ and $c^3\Pi_g$ states are studied quantum-mechanically. Theoretical and experimental data are used to characterize the molecular properties taking advantage of knowledge recently obtained from *ab initio* calculations, spectroscopy, and ultra-cold atom collision studies. The quantum-mechanical calculations are carried out for temperatures in the range from 500 to 3000 K and are compared with previous calculations and measurements where available.

PACS numbers: 33.20.-t, 34.20.Mq, 52.25.Qt

I. INTRODUCTION

Vast amounts of experimental spectroscopic data on the electronic states and ro-vibrational levels of the sodium dimer are available and many theoretical studies have been performed. For example, Ref. [1] presents an extensive bibliography summarizing a variety of work dating from 1874 to 1983. Nevertheless, recent developments in atom trapping and cold atom spectroscopy have led to improved atomic and molecular data through combinations of cold collision data, photoassociation spectroscopy, and magnetic field induced Feshbach resonance data [2–8].

Now that very reliable information is available, calculations of absorption spectra at high temperatures become feasible. Absorption coefficients in absolute units for a gas of sodium atoms and molecules at temperatures from 1070 to 1470 K were measured over the range of wavelengths from 350 to 1075 nm by Schlejen *et al.* [9]. They performed semiclassical calculations involving the relevant molecular singlet and triplet transitions, however, those previous calculations do not fully reproduce their experimental spectra [9]. The present work is concerned with the absorption involving two ground Na (3s) atoms and a ground Na (3s) atom and an excited Na (3p) atom, corresponding to transitions between the singlet transitions from the $X^1\Sigma_g^+$ state to the $A^1\Sigma_u^+$ and $B^1\Pi_u$ states and the triplet transitions from the $a^3\Sigma_u^+$ to the $b^3\Sigma_g^+$ and $c^3\Pi_g$ states. We assembled and evaluated the available data for the molecular system and calculated quantum-mechanically the absorption spectra at temperatures between 500 and 3000 K.

II. ABSORPTION COEFFICIENTS

The thermally averaged absorption coefficients k_ν for molecular spectra at wavelength ν are obtained from the product of the thermally averaged cross sections and the molecular density [10]. In turn, the molecular density can be expressed in terms of the atomic density squared and the chemical equilibrium constant [11]. In the present study, we use the atomic density-independent reduced absorption coefficient, $\frac{k_\nu}{n_a^2}$, where n_a is atomic density.

Four possible types of vibrational transitions between two electronic states can be identified: bound-bound (bb), bound-free (bf), free-bound (fb) and free-free (ff) and quantum-mechanical expressions for the reduced absorption coefficient can be derived. The radial wave function ϕ for a bound level, with vibrational and rotational quantum numbers, v and J , is obtained from the Schrödinger equation for the relative motion of the nuclei,

$$\frac{d^2\phi_{vJ\Lambda}(R)}{dR^2} + \left(2\mu E_{vJ\Lambda} - 2\mu V(R) - \frac{J(J+1) - \Lambda^2}{R^2} \right) \phi_{vJ\Lambda}(R) = 0, \quad (1)$$

where $V(R)$ is the potential for the relevant electronic state labeled by the projection Λ of the electronic orbital angular momentum on the internuclear axis, μ is the reduced mass of the nuclei, and E is the eigenvalue of the bound level or the continuum energy.

For the temperatures of interest here, $T \leq 3000$ K, the bound-bound reduced absorption coefficient from a vibration-rotation state of the lower electronic state (v'', J'', Λ'') to the vibration-rotation state of the upper electronic state (v', J', Λ') is [10,12–14]

$$\begin{aligned} \frac{k_\nu^{bb}}{n_a^2} &= \frac{C(\nu)}{h} f(k_B T) \exp(D_e/k_B T) \\ &\times \sum_{v''} \sum_{J''} \omega_{J''} (2J'' + 1) \exp(-E_{v''J''}/k_B T) |\langle \phi_{v''J''\Lambda''} | D(R) | \phi_{v'J'\Lambda'} \rangle|^2 g(\nu - \bar{\nu}), \end{aligned} \quad (2)$$

where ν is the frequency, $\bar{\nu}$ is the transition energy of the bound-bound transition,

$$C(\nu) = \frac{(2 - \delta_{0,\Lambda'+\Lambda''})}{2 - \delta_{0,\Lambda''}} \frac{8\pi^3\nu}{3c} \quad (3)$$

and [15]

$$f(k_B T) = \frac{(2S_m + 1)}{(2S_a + 1)^2} \left[\frac{h^2}{2\pi\mu k_B T} \right]^{3/2}, \quad (4)$$

S_m and S_a are spin multiplicities for, respectively, the Na molecule and the Na atom, and k_B is Boltzmann constant. The Q -branch approximation ($J' = J''$) is used and the line-shape function $g(\nu - \bar{\nu})$ is replaced by $1/\Delta\nu$. In evaluating Eq. (2) at some ν_i on the discretized frequency interval, all transitions within the frequency range $\nu_i - \frac{1}{2}\Delta\nu$ to $\nu_i + \frac{1}{2}\Delta\nu$ are summed to give a value $\frac{k_\nu^{bb}(\nu_i)}{n_a^2}$. The nuclear spin statistical factor ω_J for $^7\text{Na}_2$ with $I = \frac{3}{2}$ is $[I/(2I+1)] = \frac{3}{8}$ for even J and $[(I+1)/(2I+1)] = \frac{5}{8}$ for odd J .

The bound-free absorption coefficient from a bound level of the lower electronic state $(v''J''\Lambda'')$ to a continuum level of the upper electronic state $(\epsilon'J'\Lambda')$ is

$$\begin{aligned} \frac{k_\nu^{bf}}{n_a^2} &= C(\nu) f(k_B T) \exp(D_e/k_B T) \\ &\times \sum_{v''} \sum_{J''} \omega_{J''} (2J'' + 1) \exp(-E_{v''J''}/k_B T) |\langle \phi_{v''J''\Lambda''} | D(R) | \phi_{\epsilon'J'\Lambda'} \rangle|^2. \end{aligned} \quad (5)$$

The continuum wave function is energy normalized. For a free-bound transition and free-free transition, respectively,

$$\begin{aligned} \frac{k_\nu^{fb}}{n_a^2} &= C(\nu) f(k_B T) \\ &\times \sum_{v'} \sum_{J'} \omega_{J'} (2J' + 1) \exp(-\epsilon'/k_B T) |\langle \phi_{\epsilon'J'\Lambda'} | D(R) | \phi_{v'J'\Lambda'} \rangle|^2 \end{aligned} \quad (6)$$

and

$$\frac{k_{\nu}^{ff}}{n_a^2} = C(\nu) f(k_B T) \times \sum_{J'} \int d\epsilon' \omega_{J''} (2J'' + 1) \exp(-\epsilon''/k_B T) |\langle \phi_{\epsilon'' J'' \Lambda''} | D(R) | \phi_{\epsilon' J' \Lambda'} \rangle|^2. \quad (7)$$

III. MOLECULAR DATA

The adopted singlet $X^1\Sigma_g^+$, $A^1\Sigma_u^+$, and $B^1\Pi_u$ potentials and the differences of the upper potential and the lower $X^1\Sigma_g^+$ potential (difference potentials or transition energies) are plotted in Fig. 1. The adopted triplet $a^3\Sigma_u^+$, $b^3\Sigma_g^+$, and $c^3\Pi_g$ potentials and the difference potentials are plotted in Fig. 2. In the remainder of the section details on the construction of the potentials are given. We use atomic units throughout.

A. The $X^1\Sigma_g^+$ potential

For $R < 4 a_0$, we adopted a short range form $a \exp(-bR)$, with $a = 2\,702\,514.0 \text{ cm}^{-1}$ and $b = 2.797\,131 \text{ \AA}^{-1}$ as given by Zemke and Stwalley [16]. Over the range of $4 < R < 30 a_0$ we used the Inverse Perturbation Analysis (IPA) potential given by van Abeelen and Verhaar [7] which is consistent with data from photoassociation spectroscopy, molecular spectroscopy, and magnetic-field induced Feshbach resonances in ultra-cold atom collisions. For the long range form, we used

$$-C_6/R^6 - C_8/R^8 - C_{10}/R^{10} - AR^{\frac{7}{2}\alpha-1} \exp(-2\alpha R), \quad (8)$$

where $C_6 = 1\,561$ [2], $C_8 = 111\,877$, $C_{10} = 11\,065\,000$ [17], $A = \frac{1}{80}$, and $\alpha = 0.626$ [7,18]. To fit the very accurate dissociation energy, $6\,022.0286(53) \text{ cm}^{-1}$, recently measured by Jones *et al.* [19], a point at the potential minimum $5.819\,460 a_0$ was added. The short and long-range data were smoothly connected to the IPA values. Vibrational eigenvalues calculated with our adopted potential agree for $v \leq 44$ to within 0.1 cm^{-1} with published Rydberg-Klein-Rees (RKR) values [16]. Our final potential yielded an s -wave scattering length of $15 a_0$ in satisfactory agreement with the accepted value of $19.1 \pm 2.1 a_0$ [7].

B. The $A^1\Sigma_u^+$ potential

We used *ab initio* calculations given by Konowalow *et al.* [20] for values of R over the range $3.8 a_0 < R < 4.75 a_0$. We combined the RKR potential values over the range

2.522 19 Å < R < 7.204 14 Å given by Gerber and Möller [21] with the RKR potential values over the range of 7.260 536 Å < R < 261.327 403 Å given by Tiemann, Knöckel, and Richling [22,23]. The data was connected to the long range form,

$$-C_3/R^3 - C_6/R^6 - C_8/R^8, \quad (9)$$

with the values of $C_3 = 12.26$, $C_6 = 4094$ and $C_8 = 702\,500$ [24]. For $R < 3.8\,a_0$, the form $a \exp(-bR) + c$ was used with the parameters $a = 0.9532$, $b = 0.5061$ and $c = 0.104696$ computed to smoothly connect to the RKR points. The adopted potential yields a value of $D_e = 8\,297.5\,\text{cm}^{-1}$ using $T_e = 14\,680.682\,\text{cm}^{-1}$ [21] and the atomic asymptotic energy of $16\,956.172\,\text{cm}^{-1}$ [25]. The calculated eigenvalues reproduce the input RKR values to within $0.4\,\text{cm}^{-1}$. For the transition frequencies measured by Verma, Vu, and Stwalley [26] and by Verma *et al.* [1] over a range of vibrational bands we find typical agreement to about $0.4\,\text{cm}^{-1}$ for J' values up to 50 increasing to $1\,\text{cm}^{-1}$ for $J' = 87$. We also have good agreement with less accurate measurements by Itoh *et al.* [27]. One precise transition energy measurement is available: In a determination of the dissociation energy of the sodium molecule Jones *et al.* [19] measured the value $18762.3902(30)\,\text{cm}^{-1}$ for the $v' = 165, J' = 1$ to $v'' = 31, J'' = 0$ transition energy. Our value of $18762.372\,\text{cm}^{-1}$ is in excellent agreement.

C. The B $^1\Pi_u$ potential

The RKR potential of Kusch and Hessel [28] was used¹ over the range of $2.655\,5671\,\text{Å} < R < 5.173\,5134\,\text{Å}$. For the values of R in the ranges $2.581\,\text{Å} < R < 2.646\,0268\,\text{Å}$ and $5.251\,9184\,\text{Å} < R < 11.0\,\text{Å}$, we took the potential values from Tiemann [30]. We also took his long-range form,

$$C_3/R^3 - C_6/R^6 + C_8/R^8 - a \exp(-bR), \quad (10)$$

with $C_3 = 6.1486$, $C_6 = 6490.5$, $C_8 = 868135.2$, $a = 23.7011$, and $b = 0.7885$. For $R < 2.581\,\text{Å}$, the form $a \exp(-bR) + c$ was used with the values $a = 14.97332$, $b = 1.42983$ and $c = 0.0121935$ chosen to give a smooth connection with the data from Tiemann.

The B $^1\Pi_u$ potential exhibits a barrier that has been studied extensively [21,29–31] and the maximum value occurs around $R = 13\,a_0$ (6.9 Å) as shown in Fig. 1. We took $D_e =$

¹ For this reference, we correct an apparent typographical error of $4.309\,78\,\text{Å}$ with $4.339\,78\,\text{Å}$ obtained by comparison with RKR potential of Demtröder and Stock [29].

2676.16 cm⁻¹ using $T_e = 20\,319.19$ cm⁻¹ from Kusch and Hessel [28] and the barrier energy 371.93 cm⁻¹ measured from dissociation given by Tiemann [30]. The calculated energy 23 393.524 cm⁻¹ of the $v' = 31$, $J' = 42$ state with respect to the X $^1\Sigma_g^+$ state potential minimum compares well to the measured value, 23 393.650 cm⁻¹. Quasibound levels from $v' = 24$ to $v' = 33$ for the several J' values observed by Vedder *et al.* [32] are reproduced to within 0.1 cm⁻¹ and calculated transition frequencies compare well, to within 0.5 cm⁻¹, with those measured by Camacho *et al.* [33].

D. The a $^3\Sigma_u^+$ potential

RKR potentials are available from Li, Rice, and Field [34] and Friedman-Hill and Field [35] and a hybrid potential was constructed by Zemke and Stwalley [16] using various available data. An accurate *ab initio* study was carried out by Gutowski [3] for R values between 2 and 12.1 Å and the resulting potential has well depth 176.173 cm⁻¹ and equilibrium distance 5.204 Å.

Our adopted potential consists of Gutowski's potential connected to the long-range form given in Eq. (8) with the values for C_6 , C_8 , C_{10} and α the same as for the X $^1\Sigma_g^+$ state, but with $A = -\frac{1}{80}$. For $R < 2$ Å the short range form $a \exp(-bR)$ was used with $a = 1.4956$ and $b = 0.79438$ chosen to smoothly connect to the *ab initio* data. Our adopted potential yields an s-wave scattering length of 65 a_0 in agreement with the value 65.3 ± 0.9 of van Abeleen and Verhaar [7]. Recently, a potential alternative to Gutowski's was presented by Ho *et al.* [36]. For the present study the two potentials are comparable—we will explore their differences in a subsequent publication.

E. The b $^3\Sigma_g^+$ and c $^3\Pi_g$ potentials

We are unaware of empirical excited state triplet potentials but *ab initio* calculations are available from Magnier *et al.* [37], Jeung [38] and Konowalow *et al.* [20]. Comparing the available potentials, we found for the b $^3\Sigma_g^+$ state that the experimentally [39] determined T_e of 18 240.5 cm⁻¹ and D_e of 4 755 cm⁻¹ are closest to Magnier's calculated values (T_e of 18 117 cm⁻¹ and D_e of 4 740.7 cm⁻¹) compared with Jeung's (T_e of 18 400 cm⁻¹ and D_e of 4 702.4 cm⁻¹) and Konowalow *et al.*'s (D_e of 4 599 cm⁻¹). Also, we found Magnier's potential gave the best agreement with experimental measurements [40] of the term differences of the a $^3\Sigma_u^+(v'') \rightarrow$ b $^3\Sigma_g^+(v')$ vibrational transitions. For the b $^3\Sigma_g^+$ state and, in the absence of experimental data for the c $^3\Pi_g$ potential, we adopted Magnier's calculated potentials over

the range of R values $5 < R < 52 a_0$. Over the range of R values $4.25 < R < 5 a_0$, we used potentials by Konowalow *et al.* [20]. For the $b^3\Sigma_g^+$ and $c^3\Pi_g$ adopted potentials, the long-range form was taken from Marinescu and Dalgarno [24] for $R > 52 a_0$ and for $R < 4.25 a_0$, we used the form $a \exp(-bR)$ where the values are $a = 55.7864$ and $b = 1.75934$ for the $b^3\Sigma_g^+$ potential and $a = 2.67691$ and $b = 0.91547$ for the $c^3\Pi_g$ potential.

F. Transition dipole moment functions

We used for the singlet transitions the *ab initio* calculations of Stevens *et al.* [41] over the range $2 < R < 12 a_0$. For $R > 12$ the transition dipole moment functions were approximated by $a + b/r^3$, where $a = 3.5864$ and $b = 284.26$ for $X^1\Sigma_g^+ \rightarrow A^1\Sigma_u^+$ transitions and $a = 3.5017$ and $b = -142.13$ for $X^1\Sigma_g^+ \rightarrow B^1\Pi_u$ transitions. The parameter values for a were selected to match the short-range parts and those for b were from Marinescu and Dalgarno [24]. The $X^1\Sigma_g^+ \rightarrow A^1\Sigma_u^+$ dipole moment function was scaled with a factor of 1.008, as discussed in Sec. IV A below. For the triplet transitions the *ab initio* calculations of Konowalow *et al.* [42] were used over the range $4 < R < 100 a_0$.

IV. RESULTS

A. Lifetimes

In order to evaluate our assembled potential energy and transition dipole moment data we calculated lifetimes of ro-vibrational levels of the $A^1\Sigma_u^+$ and $B^1\Pi_u$ states and compare with prior studies.

Lifetimes for levels of the $A^1\Sigma_u^+$ state have been measured [26,43–45] and calculated [26,46]. In Fig. 3 we present a comparison of rotationally resolved lifetimes for levels of the $A^1\Sigma_u^+$ state measured by Baumgartner *et al.* [45] with the present calculations. In evaluating the lifetimes, we used the procedures described in Ref. [10]. When the transition dipole moment function of Ref. [41] is multiplied by a factor of 1.008, agreement is generally very good over the range 0 to 3500 cm^{-1} of available term energies. Our calculations are also in good agreement with the rotationally unresolved measurement of Ducas *et al.* [43] and the calculations using different molecular data by Pardo [46].

Rotationally resolved lifetimes for the $B^1\Pi_u$ state have been measured by Demtröder *et al.* [47]. Demtröder *et al.* found that the lifetimes for the $B^1\Pi_u$ state are sensitive to the slope of the transition dipole moment function in the range of internuclear separation

from, roughly, $4 < R < 10 a_0$ and they obtained an empirical value for the function that we found to be in good agreement with the transition dipole moment function of Stevens *et al.* [41]. Using the transition dipole moment function of Stevens *et al.*, in turn, we find good agreement between our calculated lifetimes and experimental lifetime measurements [47], as shown in Fig. 4. The *ab initio* dipole moment of Konowalow *et al.* [42] was found not to reproduce the experimental lifetimes.

B. Absorption Coefficients

Absorption spectra in the far-line wings of the Na(3s)-Na(3p) resonance lines are investigated in terms of singlet and triplet molecular transitions. The blue wing consists of radiation from $X^1\Sigma_g^+ \rightarrow B^1\Pi_u$ and $a^3\Sigma_u^+ \rightarrow c^3\Pi_g$ transitions and the red wing from $X^1\Sigma_g^+ \rightarrow A^1\Sigma_u^+$ and $a^3\Sigma_u^+ \rightarrow b^3\Sigma_g^+$ transitions. There are few experimental studies [9,14,48] and that of Schlejen *et al.* [9] is most relevant to our work. In this section, we compare our calculated absorption coefficients with the measurements of Schlejen *et al.* [9].

The theoretical spectra are assembled from four molecular band spectra over the wavelength range 450–1000 nm excluding the region 589 ± 2 nm around the atomic resonance lines. The far line wings are calculated using Eqs. (2)–(7), with the data from Sec. III. In the calculations, all the vibrational levels including quasi-bound levels with rotational quantum numbers up to 250 are included. The maximum internuclear distance that is used for integration of the transition dipole matrix element is approximately $100 a_0$ and the Numerov integration used to obtain the energy-normalized continuum wave function is carried out to $100 a_0$ at which the wave function is matched to its asymptotic form. The bin size $\Delta\nu$ used for Eq. (2) was 10 cm^{-1} simulating the experimental resolution. Results for absolute absorption coefficients computed with the quoted atomic densities and temperatures of Schlejen *et al.* [9] and shown in Fig. 5 compare very well with the four experimental spectra given by Schlejen *et al.*, given in Figure. 5 of Ref. [9]. The spectra show clearly that as temperature increases, certain satellite features grow more apparent at 551.5 nm and 804 nm. These satellites will be discussed in greater detail later in this section. The present calculations reproduce fine-scale ro-vibrational features present but unresolved in the measurements of Ref. [9].

We also have calculated reduced absorption coefficients at temperatures up to 3000 K using the bin size $\Delta\nu$ of 1 cm^{-1} for Eq. (2). The contributions of the four molecular bands to the reduced absorption coefficients are shown in Fig. 6 for three temperatures 1000 K, 2000 K and 3000 K. As can be seen by comparing columns (a) and (b) in Fig. 6, the singlet

transitions contribute more to the reduced absorption coefficients in the far line wings and the triplet transitions contribute more near the atomic resonance lines. We found that for singlet transitions bound-bound and bound-free transitions are dominant over free-bound and free-free transitions for the temperature range $T \leq 3000$ K, thus accounting for the “grassy” structure in Fig. 6(a). However, the free-bound and free-free contributions increase rapidly with temperature. In contrast to the singlet transitions, the triplet transitions arise mainly from free-bound and free-free transitions due to the shallow well of the initial $a^3\Sigma_u^+$ state. Hence, the reduced absorption coefficients in Fig. 6(b) do not exhibit much structure. Because the density of bound molecules decreases rapidly with increasing temperature, the reduced absorption coefficient in the line wings due to the singlet transitions also decreases rapidly with increasing temperature. It should be noted that the scale of the reduced absorption coefficient at 1000 K is two orders of magnitude larger than the scale shown for $T = 2000$ K and 3000 K.

Woerdman and De Groot [48] derived the reduced absorption coefficient at 2000 K from a discharge spectra. The measured values of $5 \pm 1 \times 10^{-37} \text{ cm}^{-1}$ at 500 nm and $10 \pm 1 \times 10^{-37} \text{ cm}^{-1}$ at 551.5 nm are well-reproduced by our values of, respectively, $5 \times 10^{-37} \text{ cm}^{-1}$ and $11 \times 10^{-37} \text{ cm}^{-1}$ calculated with the bin size $\Delta\nu$ of 5 cm^{-1} simulating the experimental resolution obtained by Woerdman and De Groot [48].

The molecular absorption spectra contain “satellite” features around the energies where the difference potentials possess local extrema [49,50]. For Na_2 the satellite frequencies have been studied [9,14,48,51] and the energies have been calculated using *ab initio* methods [42]. In the present work, we investigate the satellites arising from $a^3\Sigma_u^+ \rightarrow c^3\Pi_g$, $X^1\Sigma_g^+ \rightarrow A^1\Sigma_u^+$, and $a^3\Sigma_u^+ \rightarrow b^3\Sigma_g^+$ transitions with measured maximum intensities at, respectively, the wavelengths 551.5 nm, 804 nm, and 880 nm. The calculated extrema of the difference potentials adopted in the present study occur at wavelengths at 548 nm, 809 nm and 913 nm, however in the quantum-mechanical approach there is no well-defined singularity.

We can use the quantum-mechanical theory to study satellite features in more detail and as a function of temperature. In Fig. 7 we show calculated reduced absorption coefficients at three temperatures for the $a^3\Sigma_u^+ \rightarrow c^3\Pi_g$ and $X^1\Sigma_g^+ \rightarrow A^1\Sigma_u^+$ transitions. The rich ro-vibrational structure in the $X^1\Sigma_g^+ \rightarrow A^1\Sigma_u^+$ satellite feature arises because the dominant contributions are from bound-bound transitions; the structure is not reproduced by semi-classical theories [9]. In contrast, the smooth, structureless $a^3\Sigma_u^+ \rightarrow c^3\Pi_g$ satellite feature is due mainly to free-free transitions, and consequently, the decrease of the satellite intensity with temperature is less severe. The slight discrepancy between the calculated wavelength of 550 nm and the measured wavelength of 551.5 nm [48,52,53] for the peak intensity is

probably due to remaining uncertainties in the triplet potentials [36,54].

We also investigated the $a^3\Sigma_u^+ \rightarrow b^3\Sigma_g^+$ satellite which is far weaker in intensity at $T \leq 3000$ K than the $X^1\Sigma_g^+ \rightarrow A^1\Sigma_u^+$ and $a^3\Sigma_u^+ \rightarrow c^3\Pi_g$ satellites. The $a^3\Sigma_u^+ \rightarrow b^3\Sigma_g^+$ satellite arises primarily from free-bound transitions. The population density of atom pairs with high continuum energies in the initial $a^3\Sigma_u^+$ state increases with temperature, see Eq. (6), and more ro-vibrational levels in the $b^3\Sigma_g^+$ state are accessible through absorption of radiation, as can be seen from the potential curves shown in Fig. 2(a). As a result, this satellite feature exhibits an increase in intensity with temperature. In Fig. 8 calculated absorption coefficients for temperatures 1000, 1500, 2000 and 3000 K are plotted. The satellite feature intensity was measured at 1470 K by Schlejen *et al.* [9]. They observed a primary peak at 880 nm and a secondary peak at 850 nm, compared to our calculated values at 1500 K of 890 nm and 860 nm, respectively. The 10 nm discrepancy in both peaks is probably a result of uncertainties in the short range parts of our adopted $a^3\Sigma_u^+$ and $b^3\Sigma_g^+$ potentials. Our calculations also demonstrate that the wavelengths of the peaks change with temperature, see Fig. 8, and that the primary peak from quantum-mechanical calculations is less prominent than that obtained from semiclassical calculations exhibited in Figures 6(c) and 6(d) of Schlejen *et al.* [9]. Our calculated reduced absorption coefficients appear to be in excellent agreement with the reduced absorption coefficients interpolated from Figures 6(a) and 6(b) of Schlejen *et al.* [9] using their quoted Na densities.

V. CONCLUSIONS

We have carried out quantum-mechanical calculations of the reduced absorption coefficients in sodium vapor at high temperatures. Accurate molecular data are an important ingredient. Comparisons with experiments [9,48] are good, but the theory is not limited by the previous experimental resolution. Future work [55] will focus on comparisons of the present theory and experiments currently on-going in our group [56].

ACKNOWLEDGMENTS

We thank R. Côté and A. Dalgarno for helpful communications and E. Tiemann for generously supplying us with additional unpublished data. We are grateful to Dr. G. Lister, Dr. H. Adler, and Dr. W. Lapatovich of OSRAM SYLVANIA Inc. and Dr. M. Shurgalin, Dr. W. Parkinson, and Dr. K. Yoshino for helpful discussions. This work is supported in part by the National Science Foundation under grant PHY97-24713 and by a grant to the

Institute for Theoretical Atomic and Molecular Physics at Harvard College Observatory and
the Smithsonian Astrophysical Observatory.

FIGURES

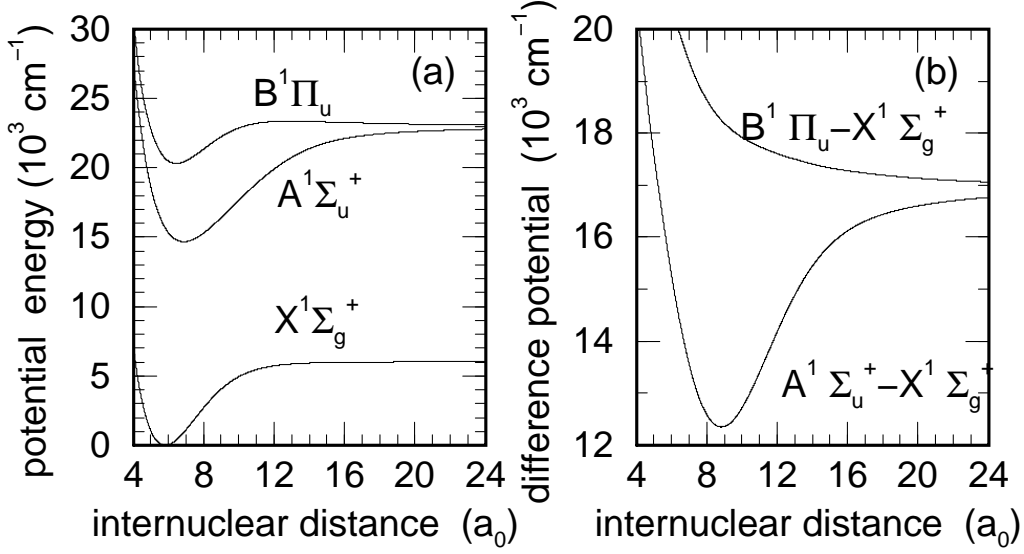


FIG. 1. (a) Adopted potentials $V(R)$ for the $X^1\Sigma_g^+$, $A^1\Sigma_u^+$, and $B^1\Pi_u$ electronic states. (b) Difference potentials $V_{B^1\Pi_u}(R) - V_{X^1\Sigma_g^+}(R)$ and $V_{A^1\Sigma_u^+}(R) - V_{X^1\Sigma_g^+}(R)$.

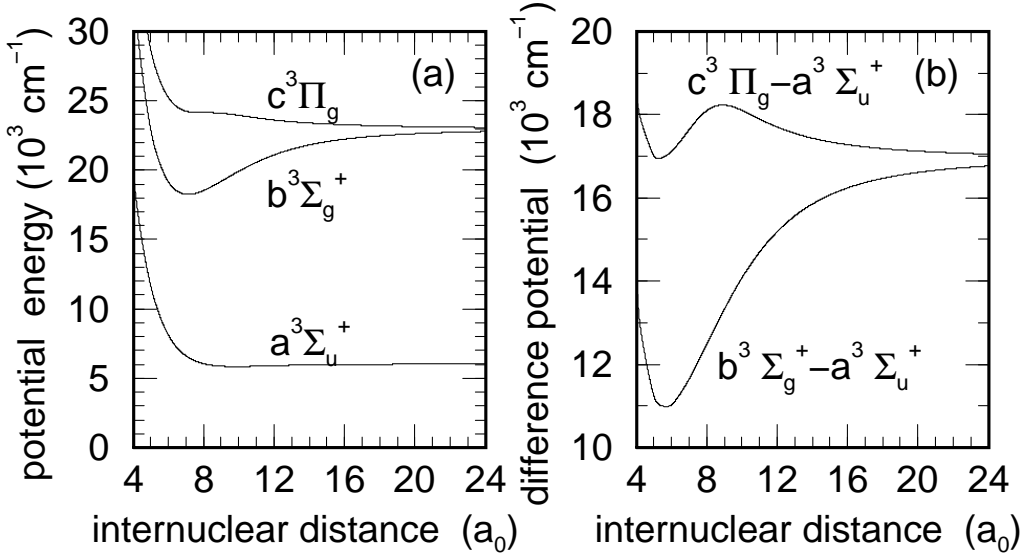


FIG. 2. (a) Adopted potentials $V(R)$ for the $a^3\Sigma_u^+$, $b^3\Sigma_g^+$ and $c^3\Pi_g$ states. (b) Difference potentials $V_{b^3\Sigma_g^+}(R) - V_{a^3\Sigma_u^+}(R)$ and $V_{c^3\Pi_g}(R) - V_{a^3\Sigma_u^+}(R)$.

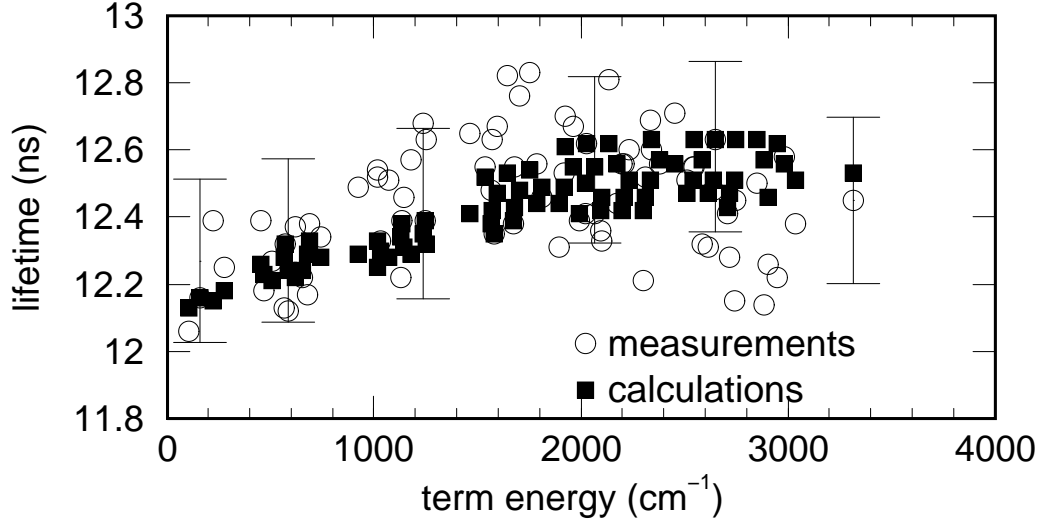


FIG. 3. Comparisons of calculated lifetimes of $A^1\Sigma_u^+$ ro-vibrational levels with experimental measurements [45].

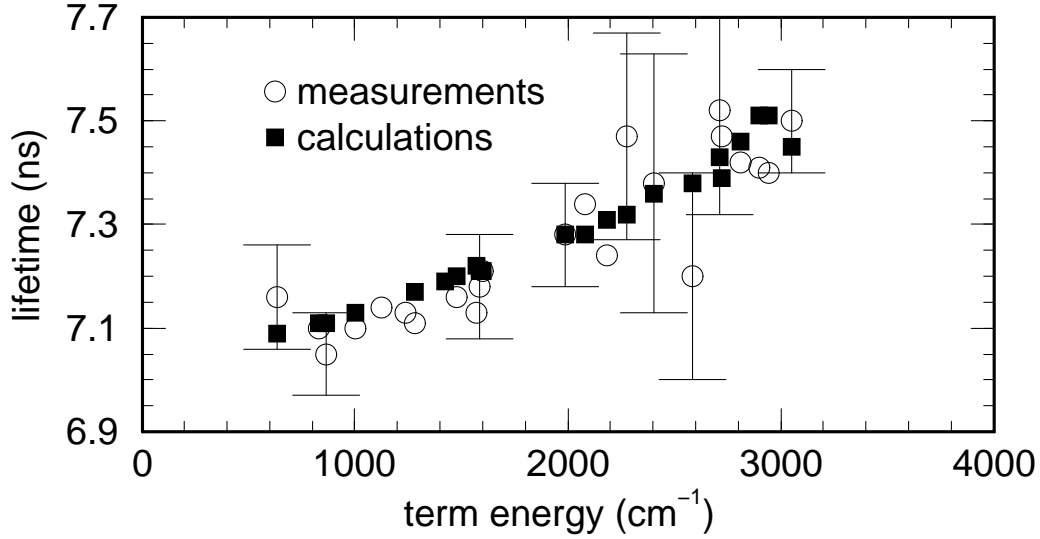


FIG. 4. Comparisons of calculated lifetimes of $B^1\Pi_u$ ro-vibrational levels with experimental measurements [47].

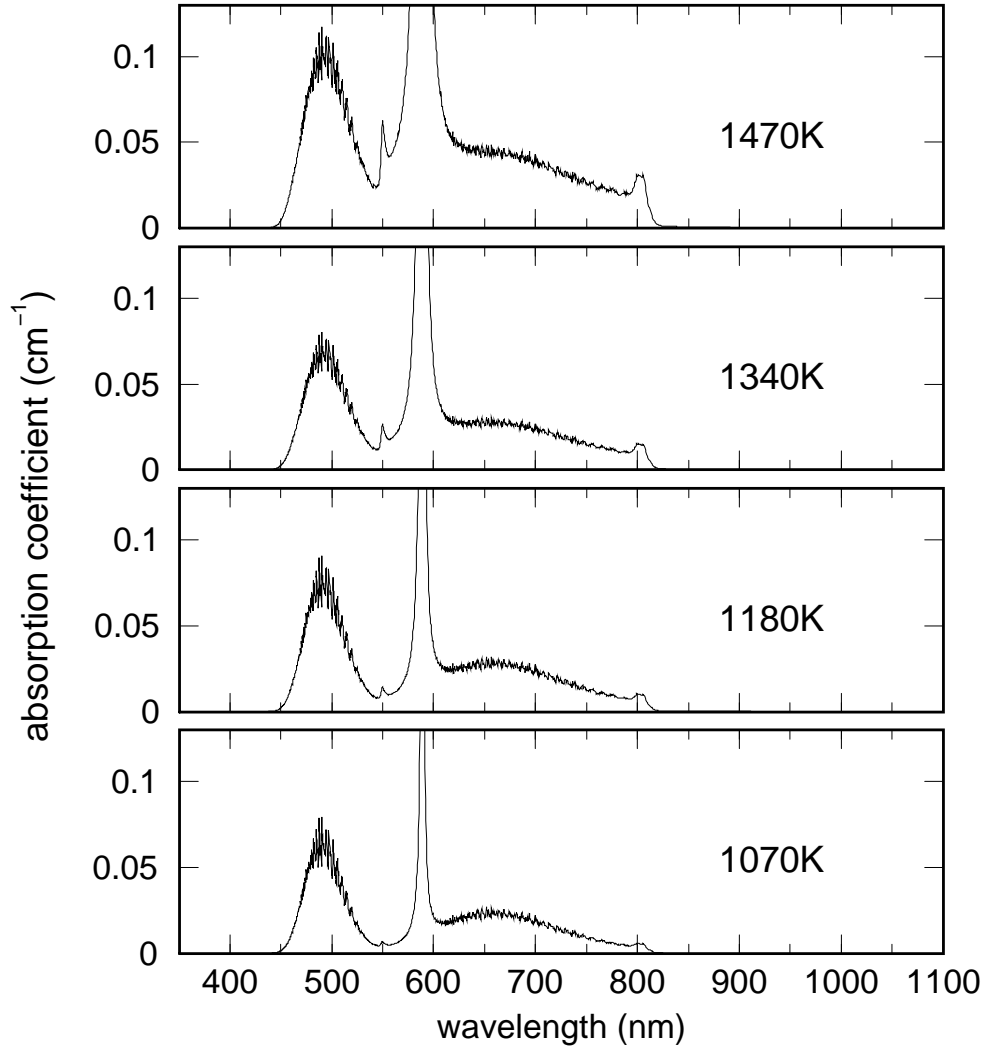


FIG. 5. Absolute values of the absorption coefficient are shown for four different temperatures for a comparison with experimental spectra reported in Figure. 5 of Ref. [9]. The calculations were performed with bin size $\Delta\nu = 10 \text{ cm}^{-1}$.

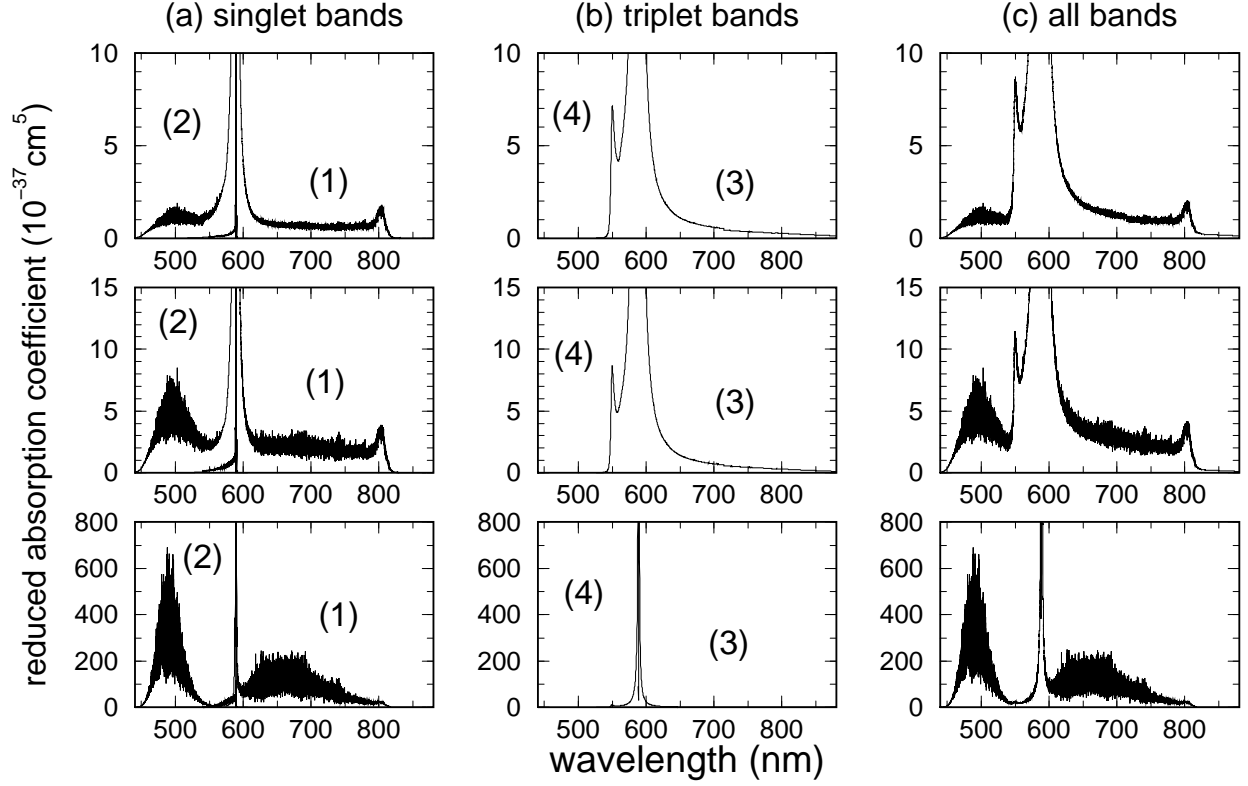


FIG. 6. Contributions to the reduced absorption coefficient at 1000 K (bottom plots), 2000 K (center plots) and 3000 K (top plots) from molecular band radiation from (a) the singlet bands, $X^1\Sigma_g^+ \rightarrow A^1\Sigma_u^+(1)$ and $X^1\Sigma_g^+ \rightarrow B^1\Pi_u(2)$ transitions, and (b) the triplet bands, $a^3\Sigma_u^+ \rightarrow b^3\Sigma_g^+(3)$ and $a^3\Sigma_u^+ \rightarrow c^3\Pi_g(4)$ transitions. The total of the singlet and triplet bands is shown in (c). Note that the scale for the reduced absorption coefficient at 1000 K is very much greater than the scale at 2000 K and 3000 K. The calculations were performed with bin size $\Delta\nu = 1 \text{ cm}^{-1}$.

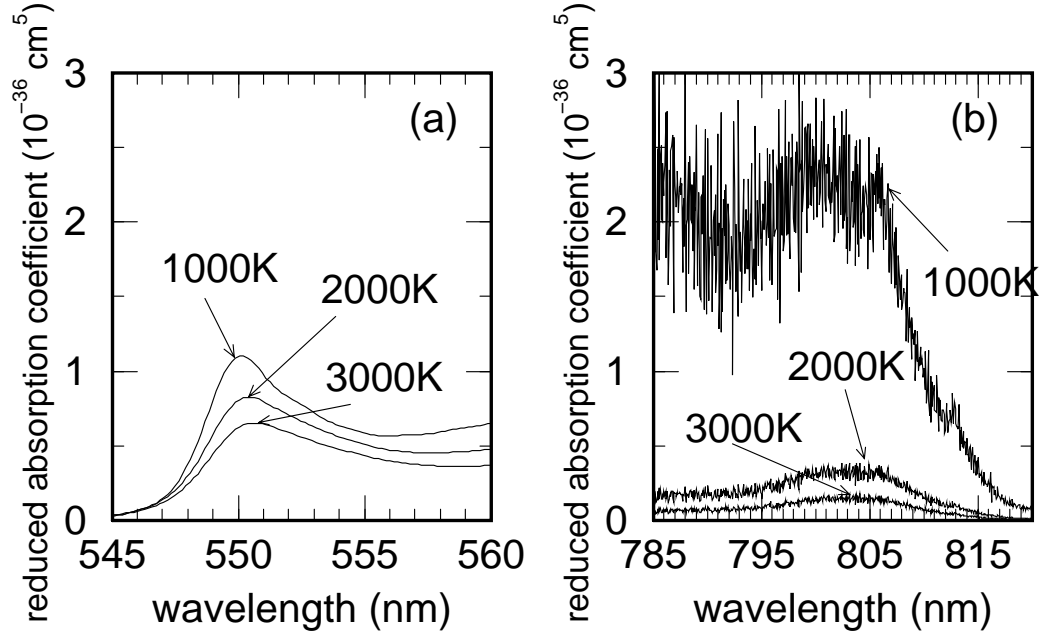


FIG. 7. (a) Calculated reduced absorption coefficients for the $a^3\Sigma_u^+ \rightarrow c^3\Pi_g$ satellite for three temperatures. (b) Calculated reduced absorption coefficients for the $X^1\Sigma_g^+ \rightarrow A^1\Sigma_u^+$ satellite for three temperatures.

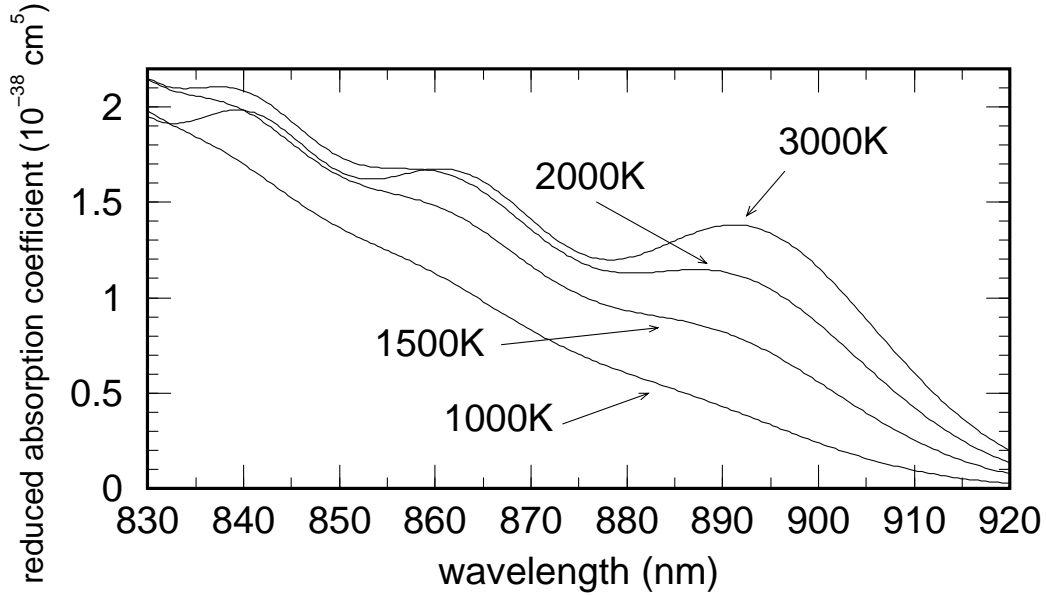


FIG. 8. Reduced absorption coefficients near satellite structures from $a^3\Sigma_u^+ \rightarrow b^3\Sigma_g^+$ bands for four temperatures. Note that the scale is two orders of magnitude smaller than in Fig. 7.

REFERENCES

- [1] K. K. Verma, J. T. Bahns, A. R. Rajaei-Rizi, and W. C. Stwalley, J. Chem. Phys. **78**, 3599 (1983).
- [2] P. Kharchenko, J. F. Babb, and A. Dalgarno, Phys. Rev. A **55**, 3566 (1997).
- [3] M. Gutowski, J. Chem. Phys. **110**, 4695 (1999).
- [4] A. J. Moerdijk and B. J. Verhaar, Phys. Rev. A **51**, R4333 (1995).
- [5] R. Côté and A. Dalgarno, Phys. Rev. A **50**, 4827 (1994).
- [6] E. Tiesinga, C. Williams, P. D. Julienne, K. M. Jones, P. D. Lett, and W. D. Phillips, J. Res. Natl. Inst. Stand. Technol. **101**, 505 (1996).
- [7] F. A. van Abeelen and B. J. Verhaar, Phys. Rev. A. **59**, 578 (1999).
- [8] A. Crubellier, O. Dulieu, F. Masnou-Seeuws, H. Knöckel, and E. Tiemann, Eur. Phys. D **6**, 211 (1999).
- [9] J. Schlejen, C. J. Jalink, J. Korving, J. P. Woerdman, and W. Müller, J. Phys. B **20**, 2691 (1987).
- [10] H.-K. Chung, K. Kirby, and J. F. Babb, Phys. Rev. A **60**, 2002 (1999).
- [11] C. Garrod, *Statistical mechanics and thermodynamics* (Oxford University Press, New York, 1995).
- [12] K. M. Sando and A. Dalgarno, Mol. Phys. **20**, 103 (1971).
- [13] R. O. Doyle, J. Quant. Spect. Rad. Trans. **8**, 1555 (1968).
- [14] L. K. Lam, A. Gallagher, and M. M. Hessel, J. Chem. Phys. **66**, 3550 (1977).
- [15] F. H. Mies and P. S. Julienne, J. Chem. Phys. **77**, 6162 (1982).
- [16] W. T. Zemke and W. C. Stwalley, J. Phys. Chem. **100**, 2661 (1994).
- [17] M. Marinescu, H. R. Sadeghpour, and A. Dalgarno, Phys. Rev. A **49**, 982 (1994).
- [18] B. M. Smirnov and M. I. Chibisov, Sov. Phys. JETP. **21**, 624 (1965).
- [19] K. M. Jones, S. Maleki, S. Bize, P. D. Lett, C. J. Williams, H. Richling, H. Knöckel, E. Tiemann, H. Wang, P. L. Gould, and W. C. Stwalley, Phys. Rev. A **54**, R1006 (1996).

- [20] D. D. Konowalow, M. E. Rosenkrantz, and D. S. Hochhauser, *J. Chem. Phys.* **72**, 2612 (1980).
- [21] G. Gerber and R. Möller, *Chem. Phys. Lett.* **113**, 546 (1985).
- [22] E. Tiemann, H. Knöckel, and H. Richling, *Z. Phys. D* **37**, 323 (1996).
- [23] E. Tiemann, 1998, private communication.
- [24] M. Marinescu and A. Dalgarno, *Phys. Rev. A* **52**, 311 (1995).
- [25] NIST Atomic Spectroscopic Database, <http://physics.nist.gov/PhysRefData/contents-atomic.html> (1999).
- [26] K. K. Verma, T. Vu, and W. C. Stwalley, *J. Mol. Spectr.* **85**, 131 (1981).
- [27] H. Itoh, Y. Fukuda, H. Uchiki, K. Yamada, and M. Matsuoka, *J. Phys. Soc. Japan* **52**, 1148 (1983).
- [28] P. Kusch and M. M. Hessel, *J. Chem. Phys.* **68**, 2591 (1978).
- [29] W. Demtröder and M. Stock, *J. Mol. Spectr.* **55**, 476 (1975).
- [30] E. Tiemann, *Z. Phys. D* **5**, 77 (1987).
- [31] J. Keller and J. Weiner, *Phys. Rev. A* **29**, 2943 (1984).
- [32] H. Vedder, G. Chawla, and R. Field, *Chem. Phys. Lett* **111**, 303 (1984).
- [33] J. J. Camacho, J. M. L. Poyato, A. M. Polo, and A. Pardo, *J. Quant. Spectrosc. Rad. Transfer* **56**, 353 (1996).
- [34] L. Li, S. F. Rice, and R. W. Field, *J. Chem. Phys.* **82**, 1178 (1985).
- [35] E. J. Friedman-Hill and R. W. Field, *J. Chem. Phys.* **96**, 2444 (1992).
- [36] T.-S. Ho, H. Rabitz, and G. Scoles, *J. Chem. Phys.* **112**, 6218 (2000).
- [37] S. Magnier, P. Millié, D. O., and F. Masnou-Seeuws, *J. Chem. Phys* **98**, 7 (1993).
- [38] G. Jeung, *J. Phys. B* **16**, 4289 (1983).
- [39] A. Färbert and W. Demtröder, *Chem. Phys. Lett.* **264**, 225 (1997).
- [40] A. Färbert, J. Koch, T. Platz, and W. Demtröder, *Chem. Phys. Lett.* **223**, 546 (1994).
- [41] W. J. Stevens, M. M. Hessel, P. J. Bertoncini, and A. C. Wahl, *J. Chem. Phys.* **66**, 1477

- (1977).
- [42] D. D. Konowalow, M. E. Rosenkrantz, and D. S. Hochhauser, *J. Mol. Spect.* **99**, 321 (1983).
 - [43] T. W. Ducas, M. G. Littman, M. L. Zimmerman, and D. Kleppner, *J. Chem. Phys.* **65**, 842 (1976).
 - [44] J. P. Woerdman, *Chem. Phys. Lett.* **53**, 219 (1978).
 - [45] G. Baumgartner, H. Kornmeier, and W. Preuss, *Chem. Phys. Lett.* **107**, 13 (1984).
 - [46] A. Pardo, preprint, 1999 (unpublished).
 - [47] W. Demtröder, W. Stetzenbach, M. Stock, and J. Witt, *J. Mol. Spect.* **61**, 382 (1976).
 - [48] J. P. Woerdman and J. J. de Groot, *Chem. Phys. Letter* **80**, 220 (1981).
 - [49] K. M. Sando and J. C. Wormhoudt, *Phys. Rev. A* **7**, 1889 (1973).
 - [50] J. Szudy and W. E. Baylis, *J. Quant. Spectr. Rad. Trans.* **15**, 641 (1975).
 - [51] J. J. de Groot, J. Schlejen, J. P. Woerdman, and M. F. M. DeKieviet, *Phillips J. Res.* **42**, 87 (1987).
 - [52] J. J. de Groot and J. A. J. M. van Vliet, *J. Phys. D* **8**, 651 (1975).
 - [53] D. Veža, J. Rukavina, M. Movre, V. Vujnović, and G. Pichler, *Opt. Comm.* **34**, 77 (1980).
 - [54] E. Tiemann, 2000, private communication.
 - [55] J. F. Babb, M. Shurgalin, H.-K. Chung, K. Kirby, W. Parkinson, and K. Yoshino, tbd, in preparation.
 - [56] M. Shurgalin, W. H. Parkinson, K. Yoshino, C. Schoene, and W. P. Lapatovich, *Meas. Sci. Technol.* **11**, 730 (2000).